FULL PAPER

BJC

British Journal of Cancer (2017) 117, 1154–1163 | doi: 10.1038/bjc.2017.298

Keywords: SKLB188; head and neck cancer; cell proliferation; apoptosis; EGF receptor; Erk1/2; Akt

SKLB188 inhibits the growth of head and neck squamous cell carcinoma by suppressing EGFR signalling

Mansoureh Barzegar[1,5], Shuang Ma[2,5], Chao Zhang[1], Xin Chen[1], Ying Gu[1], Chaowei Shang[1,3], Xiaojuan Jiang[2], Jiao Yang[2], Cherie-Ann Nathan[3,4], Shengyong Yang[*,2] and Shile Huang[*,1,3]

[1]Department of Biochemistry and Molecular Biology, Louisiana State University Health Sciences Center, 1501 Kings Highway, Shreveport, LA 71130-3932, USA; [2]State Key Laboratory of Biotherapy and Cancer Center/Collaborative Innovation Center of Biotherapy, West China Hospital, West China Medical School, Sichuan University, Chengdu, Sichuan 610041, China; [3]Feist-Weiller Cancer Center, Louisiana State University Health Sciences Center, Shreveport, LA 71130-3932, USA and [4]Department of Otolaryngology-Head and Neck Surgery, Louisiana State University Health Sciences Center, Shreveport, LA 71130-3932, USA

Background: Overexpression of epidermal growth factor receptor (EGFR) occurs in approximately 90% of head and neck squamous cell carcinoma (HNSCC), and is correlated with poor prognosis. Thus, targeting EGFR is a promising strategy for treatment of HNSCC. Several small molecule EGFR inhibitors have been tested in clinical trials for treatment of HNSCC, but none of them are more effective than the current chemotherapeutic drugs. Thus, it is urgently needed to develop novel EGFR inhibitors for HNSCC treatment.

Methods: By screening an in-house focused library containing approximately 650 000 known kinase inhibitors and kinase inhibitor-like compounds containing common kinase inhibitor core scaffolds, we identified SKLB188 as a lead compound for inhibition of EGFR. The anticancer effects of SKLB188 on HNSCC cells were investigated by *in vitro* cell growth, cell cycle and apoptosis assays, as well as *in vivo* FaDu xenograft mouse model. Molecular docking, *in vitro* kinase profiling and western blotting were performed to characterise EGFR as the molecular target.

Results: SKLB188 inhibited HNSCC cell proliferation by inducing G_1 cell cycle arrest, which was associated with downregulating the expression of Cdc25A, cyclins D1/A and cyclin-dependent kinases (CDK2/4), and upregulating the expression of cyclin-dependent kinase (CDK) inhibitors ($p21^{Cip1}$ and $p27^{Kip1}$), leading to decreased phosphorylation of Rb. SKLB188 also induced caspase-dependent apoptosis of HNSCC cells by downregulating the expression of Mcl-1 and survivin. Molecular docking revealed that SKLB188 could bind to the kinase domain of EGFR through hydrogen bonds and hydrophobic interactions. *In vitro* kinase assay showed that SKLB188 inhibited the activity of a recombinant human EGFR very potently ($IC_{50} = 5$ nM). Western blot analysis demonstrated that SKLB188 inhibited the phosphorylation of EGFR and its downstream targets, extracellular signal-regulated protein kinases 1 and 2 (Erk1/2) and Akt in the cells. In addition, SKLB188 dose-dependently inhibited FaDu xenograft growth in nude mice, and concurrently inhibited the phosphorylation of Erk1/2 and Akt in the tumours.

Conclusions: SKLB188 potently inhibits the growth of HNSCC cells *in vitro* and *in vivo* by targeting EGFR signalling. The results provide a basis for further clinical investigation of SKLB188 as a targeted therapy for HNSCC. Our findings may open a new avenue for development of novel EGFR inhibitors for treatment of HNSCC and other cancers.

*Correspondence: Dr S Huang; E-mail: shuan1@lsuhsc.edu or Professor S-Y Yang; E-mail: yangsy@scu.edu.cn
[5]These authors contributed equally to this work.

Received 2 July 2017; revised 1 August 2017; accepted 3 August 2017; published online 5 September 2017

Epidermal growth factor receptor (EGFR, also named ErbB-1 or HER1), a receptor tyrosine kinase, belongs to the ErbB superfamily, which includes three other members: ErbB2/Neu/HER2, ErbB3/HER3, and ErbB4/HER4 (Furnari *et al*, 2015). In response to the binding of ligands, for example, epidermal growth factor (EGF) and transforming growth factor α (TGFα), EGFR is homodimerised with another EGFR or heterodimerised with other ErbB family members, and activated through autophosphorylation at several tyrosine (Y) residues in its C-terminal domain. This results in the activation of multiple downstream pathways including Ras/Raf/MEK/Erk and PI3K/Akt/mTOR cascades (Furnari *et al*, 2015; Guo *et al*, 2015). Hence, EGFR plays an important role in the regulation of cell growth, proliferation, survival, migration, and differentiation (Furnari *et al*, 2015; Guo *et al*, 2015).

Aberrant activation of EGFR signalling, due to EGFR overexpression and/or mutations, has been found to be associated with the development and progression of a variety of human malignancies, such as lung, head and neck, breast, colorectal, and pancreatic cancers (Scaltriti and Baselga, 2006; Cohen, 2014). Thus, EGFR has received great attention for targeted therapy. Currently, two major approaches have been developed to inhibit EGFR: monoclonal antibodies (mAbs) (e.g., Cetuximab and Panitumumab) that block the extracellular ligand binding domain, and small molecule tyrosine kinase inhibitors (TKIs) (e.g., Gefitinib and Erlotinib) that bind the ATP binding site of the intracellular kinase domain of the receptor (Chong and Jänne, 2013).

Head and neck squamous cell carcinoma (HNSCC) is the sixth most common cancer worldwide, with over 550 000 cases and around 300 000 deaths annually (Leemans *et al*, 2011). Current standard treatment of HNSCC patients is by multimodal approaches consisting of surgery, radiotherapy, and/or chemotherapy (e.g., platinum analogues, taxanes, fluorouracil, and methotrexate) (Colevas, 2006). However, considerable side effects and drug resistance occur frequently, when patients are treated with those conventional chemotherapeutic agents (Pezzuto *et al*, 2015). As overexpression of EGFR occurs in more than 90% of HNSCC cases and is correlated to poor prognosis (Kang *et al*, 2015), targeting EGFR has been regarded as a promising strategy for treatment of HNSCC. Currently, Cetuximab, a chimeric human-murine IgG1 mAb directed specifically against EGFR, is the only US Food and Drug Administration-approved and European Medicines Agency-approved targeted therapy for HNSCC (Cohen, 2014; Sacco and Worden, 2016). However, the overall response rate of monotherapy with Cetuximab is modest, ranging from 10 to 13% (Sacco and Worden, 2016). Several oral EGFR TKIs, including Gefitinib and Erlotinib, which are clinically used for treatment of non-small cell lung cancer (NSCLC), have been tested in clinical trials in HNSCC, but none of those has been demonstrated to be more effective than the current chemotherapeutic drugs (Rodriguez *et al*, 2012; Martins *et al*, 2013; Sacco and Worden, 2016). Therefore, it is urgently needed to develop novel EGFR inhibitors for HNSCC treatment.

Recently, by screening an in-house focused library containing approximately 650 000 known kinase inhibitors and kinase inhibitor-like compounds containing common kinase inhibitor core scaffolds, we have identified that SKLB188 is a potential anticancer agent. This study was set to evaluate the anticancer activity in HNSCC cells *in vitro* and *in vivo* and to determine the molecular target of SKLB188. Here, we show that SKLB188 inhibited cell proliferation and induced apoptosis in head and neck cancer cells (FaDu and PCI-13) *in vitro*. Also, SKLB188 inhibited the growth of FaDu xenografts *in vivo*, without showing obvious toxicity in mice. Mechanistically, SKLB188 was found to inhibit EGFR-mediated MEK/Erk and Akt/mTOR signalling pathways in the HNSCC tumour cells *in vitro* and *in vivo*. Our findings suggest that SKLB188 is a novel EGFR inhibitor, which may be explored for treatment of head and neck cancer and other tumours.

MATERIALS AND METHODS

Reagents. SKLB188 was synthesised at the State Key Laboratory of Biotherapy, Sichuan University (Chengdu, China), while Iressa (Gefitinib) was obtained from LC Laboratories (Woburn, MA, USA). Both SKLB188 and Iressa were dissolved in dimethyl sulfoxide (DMSO) to prepare a stock solution (10 mM), then aliquoted and stored at −20 °C. RPMI 1640 and 0.05% Trypsin-EDTA were purchased from Mediatech (Herndon, VA, USA). Fetal bovine serum (FBS) was from Atlanta Biologicals (Lawrenceville, GA, USA). Recombinant human EGF (PeproTech, Rocky Hill, NJ, USA) was rehydrated in 0.1 M acetic acid to prepare a stock solution (100 μg ml^{-1}), aliquoted and stored at −80 °C. The following antibodies were used: CDK2, CDK4, CDK6, cyclin D1, cyclin A, Cdc25A, p21^{Cip1}, p27^{Kip1}, p-Rb (S807/811), survivin, Mcl-1, Bcl-2, Bcl-xL, BAX, BAK, BAD, Erk2, S6K1, S6, Akt (Santa Cruz Biotechnology, Santa Cruz, CA, USA), phospho-EGFR (Ser1070) (GeneTex, Irvine, CA, USA), cleaved caspase 3, cleaved PARP, EGFR, phospho-Erk1/2 (Thr202/Tyr204), phospho-Akt (Ser473), phospho-S6K1 (Thr389), phospho-S6 ribosomal protein (Ser235/236), CD31 (Cell Signaling, Danvers, MA, USA), Ki-67 (Thermo Fisher Scientific, Waltham, MA, USA), β-tubulin (Sigma-Aldrich, St Louis, MO, USA), and goat anti-mouse IgG-horseradish peroxidase, and goat anti-rabbit IgG-horseradish peroxidase (Pierce, Rockford, IL, USA). All other chemicals were obtained from Sigma-Aldrich, unless stated elsewhere.

***In vitro* kinase assay.** *In vitro* kinase inhibitory activities were measured by radiometric assays conducted by Eurofins Pharma Discovery Services UK Limited (Dundee, Scotland). Kinase profiling of SKLB188 was carried out at a fixed concentration of 10 μM. The IC_{50} values were calculated based on the dose–response data of 10 points by using Graphpad Prism (Graphpad Software, San Diego, CA, USA).

Cell culture. Human head and neck cancer cell line FaDu was obtained from American Type Culture Collection (Manassas, VA, USA). Human head and neck cancer cell line PCI-13 was described previously (Clark *et al*, 2010). FaDu and PCI-13 cells were cultured in antibiotic-free RPMI 1640 supplemented with 10% FBS. All cell lines were cultured in a humidified atmosphere at 37 °C with 5% CO_2.

Cell proliferation assay. Cell proliferation assays were conducted as described previously (Zhou *et al*, 2010). Briefly, cells, grown in six-well plates, were treated with SKLB188 (0–2 μM) for 6 days, followed by cell counting with a Z1 counter (Beckman Coulter, Fullerton, CA, USA). Cells treated with the vehicle (DMSO) alone served as a control.

MTS assay. Cell viability was evaluated using CellTiter 96 AQ_{ueous} One Solution Cell Proliferation Assay kit (Promega, Madison, WI, USA), as described previously (Zhou *et al*, 2010). Briefly, cells, grown in 96-well plates, were treated with SKLB188 (0–2 μM) for 24–72 h. Subsequently, cell viability, after incubation with MTS reagent (20 μl per well) for 3 h, was monitored by the optical density at 490 nm using Synergy 4 microplate reader (BioTek, Winooski, VA, USA). Cells treated with the vehicle (DMSO) alone served as a control.

Trypan blue exclusion assay. Cell viability was also evaluated by the trypan blue exclusion assay, as described previously (Chen *et al*, 2014). Briefly, cells were seeded in 100-mm dishes at a density of 2×10^5 cells per dish in the growth medium and grown overnight at 37 °C in a humidified incubator with 5% CO_2. Following treatment with SKLB188 (0–2 μM) for 24–72 h, the cells (including floating and attached cells) were collected, pelleted, and resuspended in 1 ml of PBS. Then, one part of cell suspension was

incubated with one part of 0.4% trypan blue solution (Sigma) for 3 min at room temperature. Finally, 10 μl of the trypan blue/cell mixture was applied to a hemacytometer, and the unstained (viable) and stained (nonviable) cells were counted separately under a microscope. For each treatment, at least 300 cells (total) were counted, and the percentage of the stained cells was calculated.

Cell cycle analysis. Cell cycle analysis was performed, as described previously (Zhou *et al*, 2010). Briefly, cells were treated with SKLB188 (0–2 μM) for 24 h, and then stained with the Cellular DNA Flow Cytometric Analysis Kit (Roche Diagnostics, Indianapolis, IN, USA). Percentages of cells within each of the cell cycle compartments (G_0/G_1, S, or G_2/M) were determined using a FACSCalibur flow cytometer (Becton Dickinson, San Jose, CA, USA) and ModFit LT analyzing software (Verity Software House, Topsham, ME, USA). Cells treated with the vehicle (DMSO) alone were used as a control.

Apoptosis assay. Cell apoptosis was determined, as described previously (Odaka *et al*, 2014). Briefly, cells were treated with SKLB188 (0–2 μM) for 72 h. Cells were then collected and stained using Annexin V-FITC Apoptosis Detection Kit I (BD Biosciences, Sparks, MD, USA), followed by flow cytometry using a FACS Calibur flow cytometer (Becton Dickinson). Cells treated with DMSO alone were used as a control.

Molecular docking. The molecular docking studies were performed using GOLD 5.0 (Jones *et al*, 1997) (Genetic Optimization of Ligand Docking, Cambridge, UK). The X-ray crystal structure (PDB entry 2J6M) of the kinase domain of EGFR (WT) bound to the compound AEE788 (Yun *et al*, 2007) was used in the docking studies. The Discovery Studio 3.1 (Accelrys, San Diego, CA, USA) software package was used to prepare the protein structure including adding hydrogen atoms to the protein, removing water molecules, and assigning force field (here the CHARMm force field was adopted). The binding site was defined as a sphere containing residues that remain within 12 Å of the ligand, an area large enough to cover the ATP-binding region at the kinase domain.

Western blot analysis. Western blotting was performed, as described previously (Luo *et al*, 2015). Briefly, equivalent amounts of proteins (whole cell lysates) were separated on 8–15% sodium dodecyl sulfate-polyacrylamide gels and transferred to polyvinylidene difluoride membranes (Millipore, Bedford, MA, USA). Membranes were blocked with 5% non-fat dry milk (dissolved in PBS containing 0.05% Tween 20) for 1 h at room temperature, and then incubated with primary antibodies overnight at 4 °C, followed by probing with appropriate secondary antibodies conjugated to horseradish peroxidase overnight at 4 °C. Immunoreactive bands were visualised by using Renaissance chemiluminescence reagent (Perkin-Elmer Life Science, Boston, MA, USA).

FaDu xenograft model. All animal experiments carried out were approved by the Animal Care and Use Committee of Sichuan University. Female 5 ~ 6-week-old Balb/c nude mice (Beijing HFK Bioscience, Beijing, China) were housed in a sterile environment and fed a standard diet *ad libitum*. FaDu cells were collected and resuspended at a concentration of 5×10^7 cells ml^{-1} in serum-free medium. Then, a 100-μl aliquot of the cell suspension was injected subcutaneously into the hind flank of each mouse. Mice were randomised into five groups when the tumours reached a volume of 150 mm^3. SKLB188 or Iressa was dissolved in 25% (v/v) PEG400 plus 5% DMSO in deionised water. Mice were orally treated with vehicle control, 12.5 mg kg^{-1} SKLB188, 25 mg kg^{-1} SKLB188, 50 mg kg^{-1} SKLB188 and 12.5 mg kg^{-1} Iressa once daily. Tumour volume [(length $\times$ width^2)/2] was determined with a digital caliper. Tumour growth and mice body weight were monitored every three days and analysed. At the end of experiments, animals were killed, and the tumours were collected, photographed, and analysed.

To study the mechanism of anti-tumour action of SKLB188 *in vivo,* when the FaDu-xenografted tumours reached a volume of 150 mm^3, mice were randomly grouped (four mice per group) and treated for 7 days with vehicle, SKLB188 (50 mg kg^{-1}), and Iressa (50 mg kg^{-1}) (as a positive control), respectively. Then, animals were killed, and the tumours were collected and evaluated by haematoxylin and eosin, TUNEL, and immunohistochemistry with indicated antibodies.

Immunohistochemistry and TUNEL staining. At the end of experiments, tumour tissues were excised and fixed with 10% neutral buffered formalin, embedded in paraffin and sectioned using a standard histological procedure. Haematoxylin and eosin staining and TUNEL staining using DeadEnd Colorimetric TUNEL System (Promega) were performed, as described previously (Zhou *et al*, 2010; Zheng *et al*, 2016). Immunohistochemical staining for Ki-67, CD31, p-Akt, p-Erk1/2, and p-S6 was conducted using corresponding antibodies, using the protocol as described (Zhou *et al*, 2010; Zheng *et al*, 2016). Quantitative analysis of TUNEL, Ki-67, CD31, p-Erk1/2, p-Akt or p-S6-positive staining was performed with NIH ImageJ software. At least four independent regions were evaluated from at least three independent mice per group.

Statistical analysis. The results were expressed as mean values ± standard error (mean ± s.e.). Statistical analysis was performed using one-way ANOVA followed by Bonferroni's post-tests. Significance was accepted at $P < 0.05$.

RESULTS

SKLB188 inhibits cell proliferation and induced cell death in HNSCC cells. To assess the anticancer activity of SKLB188 in HNSCC cells *in vitro*, first of all, we tested whether SKLB188 inhibits cell proliferation and induces cell death in FaDu and PCI-13 cells. As shown in Figure 1A, treatment with SKLB188 for 6 days inhibited cell proliferation of FaDu and PCI-13 cells in a concentration-dependent manner, with $IC_{50} = 10$–20 nM. Furthermore, treatment with SKLB188 (0–2 μM) for 24–72 h reduced the cell viability in both FaDu and PCI-13 cells in a concentration- and time-dependent manner, as detected by MTS assay (Figure 1B). As MTS assay cannot distinguish cell proliferation from cell death, trypan blue exclusion assay was utilised to verify the cytotoxicity of SKLB188. The results showed that SKLB188 did induce the cell death in FaDu cells (Supplementary Figure S1). Collectively, the results indicate that SKLB188 is a potent anticancer agent for HNSCC cells.

SKLB188 induces G_1 cell cycle arrest by downregulating the expression of cyclins D1/A, CDK2/4 and Cdc25A and upregulating the expression of CDK inhibitors in HNSCC cells. To understand how SKLB188 inhibits cell proliferation, cell cycle analysis was performed. Treatment with SKLB188 (0–2 μM) for 24 h accumulated FaDu cells at G_0/G_1 phase of the cell cycle in a concentration-dependent manner. Of note, SKLB188 at 0.1 μM was able to increase the proportion of the cells in the G_0/G_1 phase drastically from approximately 47.5 (control) to 78.5%, and correspondingly decrease the fraction of the cells in the S phase from about 42.2 (control) to 19.5%, and decrease the portion of the cells in the G_2/M phase from 10.3 to 2.3% (Figure 2A). Furthermore, we observed that SKLB188-induced G_1 cell cycle arrest sustained for up to 72 h (Figure 2B). Therefore, our results suggest that SKLB188 inhibits cell proliferation by arresting cells in G_1 phase of the cell cycle.

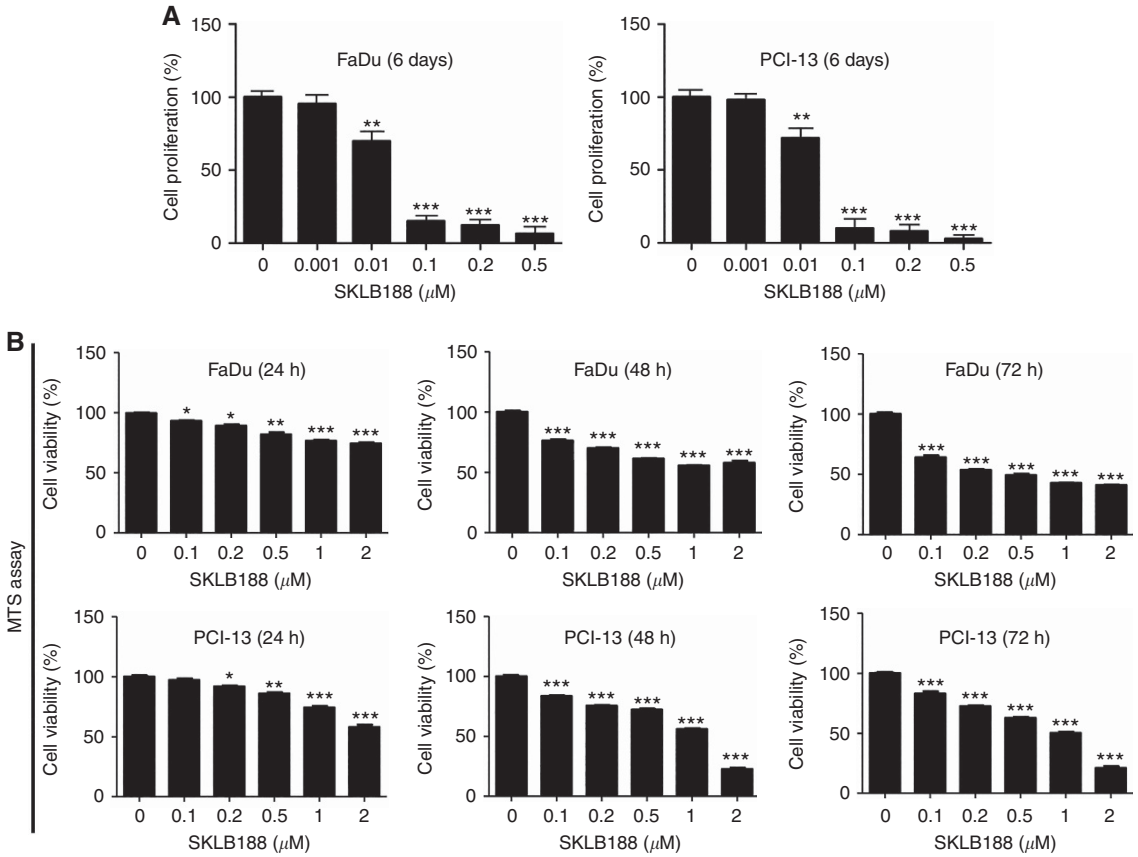

Figure 1. SKLB188 inhibits cell proliferation and induces cell death in HNSCC cells. (**A**) FaDu and PCI-13 cells were treated with SKLB188 (0–2 μM) for 6 days, followed by cell counting. (**B**) FaDu and PCI-13 cells were treated with SKLB188 (0–2 μM) for 24–72 h, followed by cell viability assay (MTS assay). All data represent the means ± s.e. ($n = 3$). *$P < 0.05$, **$P < 0.01$, and ***$P < 0.001$.

Cell proliferation is directly determined by the progression of the cell cycle, which is divided into G_0/G_1, S, and G_2/M phases, and is driven by various CDKs (Sherr and Roberts, 1999; Malumbres and Barbacid, 2009). To further unveil how SKLB188 induces G_1 cell cycle arrest, we examined the expression of CDKs and related regulatory proteins, including cyclins, Cdc25 and CDK inhibitors. As shown in Figure 2C, treatment with SKLB188 for 24 h downregulated the cellular protein expression of cyclin D1, cyclin A, CDK1, CDK2, CDK4, and Cdc25A, and upregulated the protein expression of two CDK inhibitors, $p21^{Cip1}$ and $p27^{Kip1}$, in a concentration-dependent manner. As a result, treatment with SKLB188 for 24 h reduced the phosphorylation of Rb (S780) (Figure 2B). Similar results were observed in PCI-13 cells (Figure 2D). Thus, our data suggest that SKLB188 arrested cells in G_0/G_1 phase of the cell cycle by downregulating the expression of cyclins D1/A, CDK1/2/4 and Cdc25A and upregulating the expression of CDK inhibitors ($p21^{Cip1}$ and $p27^{Kip1}$), leading to dephosphorylation of Rb.

SKLB188 induces caspase-dependent apoptotic cell death in HNSCC cells. To determine whether SKLB188 induces apoptotic cell death, we performed Annexin V-FITC/PI staining, a method that is frequently used to detect apoptosis (van Engeland *et al*, 1998). As shown in Figure 3A and B, treatment with SKLB188 for 72 h induced apoptosis in FaDu cells in a concentration-dependent manner. SKLB188 at 0.1–2 μM increased the apoptotic (Q2 late apoptotic + Q4 early apoptotic) cells by approximately 1.6–3.0-fold, compared to the control. Similar results were observed in PCI-13 cells (Supplementary Figure S2A and B).

Bcl-2 family members, including anti-apoptotic (e.g., Bcl-2, Bcl-xL, and Mcl-1) and pro-apoptotic proteins (e.g., BAD, BAK, and BAX), are key players in the regulation of apoptosis (Llambi and Green, 2001; Elmore, 2007). To understand how SKLB188 induces apoptosis, we next examined whether SKLB188 alters the expression of pro-apoptotic and anti-apoptotic proteins in the cells. As shown in Figure 3C, treatment with SKLB188 for 24 h markedly downregulated the expression levels of anti-apoptotic proteins (Mcl-1 and survivin) and meanwhile upregulated the pro-apoptotic protein BAD level in a concentration-dependent manner. Furthermore, we observed that SKLB188 induced PARP cleavage (Figure 3C), a hallmark of caspase-dependent apoptosis. This was consistent with the data that SKLB188 increased the cleavage of caspase 3 (Figure 3C), indicating activation of caspase 3. Similar results were observed in PCI-13 cells (Supplementary Figure S2C). Therefore, our results suggest that SKLB188 induces caspase-dependent apoptotic cell death by downregulating the expression of anti-apoptotic proteins Mcl-1/survivin and upregulating the expression of pro-apoptotic protein BAD in HNSCC cells.

Molecular docking predicts the binding of SKLB188 to EGFR kinase domain. To identify the molecular target of SKLB188 (Figure 4A), molecular docking studies were performed. Figure 4B illustrates that the purine ring locates at the ATP binding pocket, where it is sandwiched between the N- and C-lobes of the catalytic domain of EGFR. Three hydrogen bonds are formed between SKLB188 and the kinase domain of EGFR: the first one corresponds to that formed between the nitrogen (NH) of 2-aniline of purine and the Met793 residue in the hinge region of

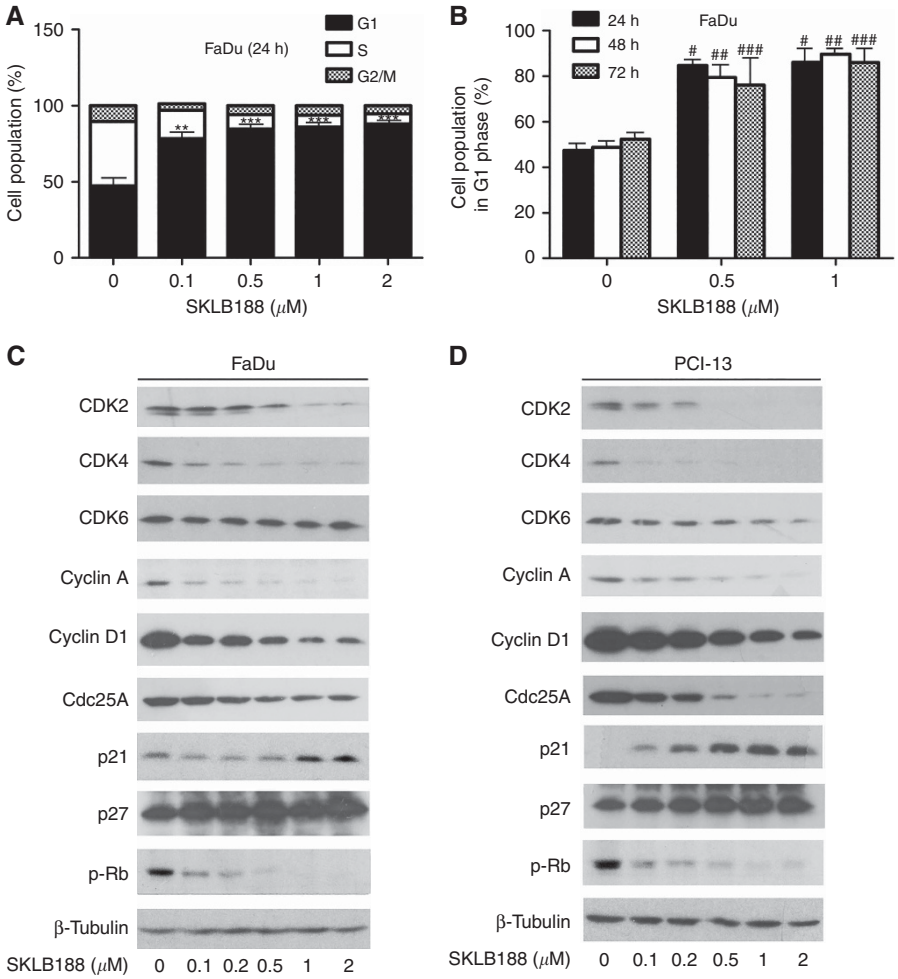

Figure 2. SKLB188 induces G_1 cell cycle arrest by downregulating the expression of cyclins D1/A, CDK2/4 and Cdc25A and upregulating the expression of CDK inhibitors ($p21^{Cip1}$ and $p27^{Kip1}$), leading to dephosphorylation of Rb. (**A** and **B**) FaDu cells were treated with SKLB188 (0–2 μM) for 24 h (**A**) or with indicated concentrations of SKLB188 for 24–72 h, followed by cell cycle analysis. All data represent the means ± s.e. ($n = 3$). For (**A**), $^{**}P<0.01$, $^{***}P<0.001$: control *vs* treatment with SKLB188 at indicated concentrations; for (**B**), $^{\#}P<0.05$, $^{\#\#}P<0.05$, $^{\#\#\#}P<0.05$: control *vs* treatment with SKLB188 for 24, 48, and 72 h, respectively. (**C** and **D**) FaDu and PCI-13 cells were exposed to SKLB188 for 24 h, followed by western blotting with indicated antibodies. Similar results were observed in at least three independent experiments.

EGFR, the second one is between N1 (namely N3 in Figure 4C) of purine and the Met793 residue, and the third one is between one of the nitro/oxygen atoms and the Lys745 residue. Additionally, the cyclopentyl group in SKLB188 forms a hydrophobic interaction with residues Leu718, Gly719, and Val726. Therefore, the above results suggest that SKLB188 has the ability to bind the EGFR kinase domain and may represent a new class of EGFR inhibitor.

SKLB188 is a multikinase inhibitor and potently inhibits EGFR. To assess the kinase inhibitory activities of SKLB188, we conducted an *in vitro* kinase inhibition profile of SKLB188 against a total of 399 recombinant human protein kinases using the 'gold standard' radiometric kinase assay. The results showed that SKLB188, when at a fixed concentration of 10 μM, was able to inhibit a number of receptor tyrosine kinases, including Abl, EGFR, Erb2, Erb4, Flt1, Flt3, Flt4, EphB, FGFR, c-Kit, Met, and PDGFR (Supplementary Table S1). Given our above molecular docking results, next, we studied the dose–response relationship of SKLB188 against the EGFR kinase. The results revealed that SKLB188 dose-dependently inhibited the EGFR activation with an IC_{50} value of 5 nM (Figure 4D). As a control, SKLB188 inhibited c-Kit activation with an IC_{50} value of 1272 nM. Thus, our *in vitro* kinase inhibition data support that SKLB188 is an EGFR inhibitor, but at higher concentrations may inhibit other RTKs.

SKLB188 inhibits EGFR signalling in HNSCC cells. The phosphorylation level of EGFR is a surrogate of EGFR activity (Keese *et al*, 2005). To determine whether SKLB188 inhibits EGFR in cells, we investigated the effect of SKLB188 on the phosphorylation of EGFR in HNSCC cells. For this, serum-starved FaDu cells were treated with SKLB188 (0–2 μM) or Iressa (as a positive control) for 24 h, followed by stimulation with EGF (50 ng ml^{-1}) for 1 h. Our western blot analysis showed that SKLB188 inhibited the phosphorylation of EGFR (S1070) in a concentration-dependent manner (Figure 5A). Interestingly, at 0.1 μM, SKLB188 showed more potent inhibitory effect on p-EGFR than Iressa. Since EGFR regulates Ras/Raf/MEK/Erk and PI3K/Akt/mTOR pathways (Scaltriti and Baselga, 2006), we also studied whether SKLB188 inhibits these two downstream pathways. As expected, treatment with SKLB188 also inhibited the phosphorylation of MEK1/2 and Erk1/2 (Figure 5A), as well as the phosphorylation of Akt, S6K1, and S6 (Figure 5B) in a concentration-dependent manner. Consistently, at low concentrations (0.1–0.5 μM), SKLB188 displayed stronger inhibitory effects on the two pathways than Iressa. Similar results were observed in PCI-13 cells

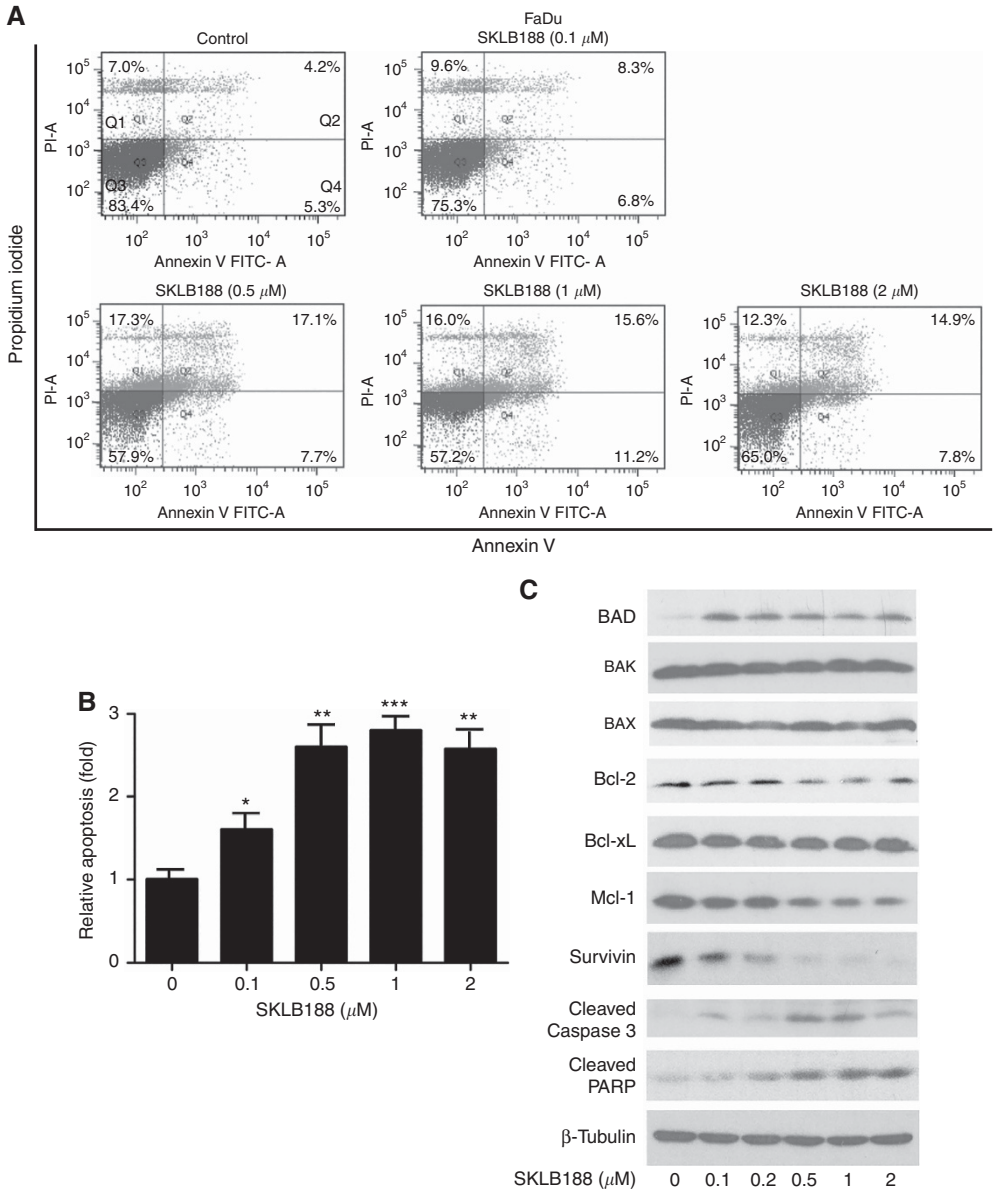

Figure 3. SKLB188 induces caspase-dependent apoptosis by downregulating the expression of Mcl-1/survivin and upregulating the expression of BAD in FaDu cells. (**A**) FaDu cells were treated with SKLB188 (0–2 μM) for 72 h, followed by Annexin V/PI staining and flow cytometry. Representative diagrams are shown. (**B**) Data from (**A**) were statistically analysed. Means ± s.e. ($n = 3$). *$P < 0.05$, **$P < 0.01$, ***$P < 0.001$. (**C**) FaDu cells were exposed to SKLB188 for 24 h, followed by western blotting with indicated antibodies. Similar results were observed in at least three independent experiments.

(Supplementary Figure S3). Thus, our data further support that SKLB188 is an inhibitor of EGFR.

SKLB188 inhibits FaDu xenograft growth in nude mice. To evaluate the anti-tumour activity of SKLB188 *in vivo*, FaDu xenograft model was used. In this model, FaDu cells were injected subcutaneously into the hind flank of each nude mouse, then the mice were randomised into five groups (6 mice per group) when the tumours grew to a size of $\sim$150 mm^3. Next, the animals were orally given three doses (12.5, 25, and 50 mg kg^{-1}) of SKLB188, one dose (12.5 mg kg^{-1}) of Iressa (positive control) or vehicle (control) every day. We found that SKLB188 dose-dependently inhibited the tumour growth (volume) by 63.5%, 88.7%, and 102.2% at doses of 12.5, 25, and 50 mg kg^{-1}, respectively, while Iressa (12.5 mg kg^{-1}) inhibited the tumour growth (volume) by 78.3% (Figure 6A) at the end of the experiment, compared with the vehicle. Similarly, treatment with SKLB188 or Iressa also inhibited the tumour weight increase significantly, compared with the vehicle treatment (Figure 6B). Of note, no obvious toxicity was observed in all the treated groups except the 50 mg kg^{-1}-SKLB188 group, in which the average body weight of mice decreased slightly but not significantly (Figure 6A).

To elucidate the mechanism of anti-tumour action of SKLB188 *in vivo*, immunohistochemical analysis was conducted using FaDu tumour samples collected from mice treated with vehicle, SKLB188 (50 mg kg^{-1}) and Iressa (50 mg kg^{-1}), respectively. As shown in Figure 6C and D, SKLB188, like Iressa, potently inhibited the phosphorylation of Erk1/2, Akt and S6, and led to a substantial decrease in tumour cell proliferation (Ki67-positive staining) and a significant increase in apoptosis (TUNEL-positive staining), compared with the vehicle. Moreover, SKLB188, like Iressa, remarkably reduced the microvessel density (CD31 staining).

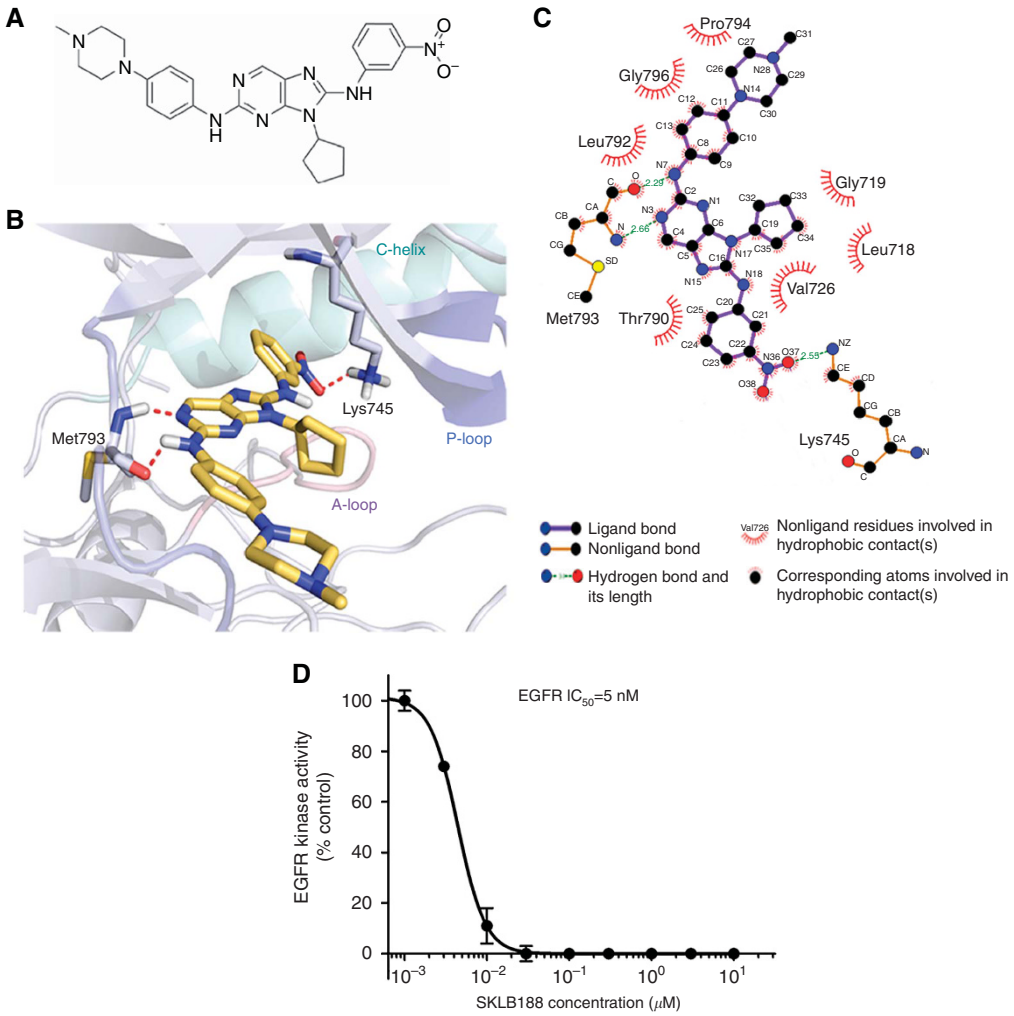

Figure 4. SKLB188 is predicted to bind the EGFR kinase domain and inhibits EGFR activity *in vitro*. (**A**) Chemical structure of SKLB188. (**B**) SKLB188 is docked into the EGFR kinase domain, showing interactions between SKLB-188 and EGFR. (**C**) A two-dimensional interaction map of SKLB188 and EGFR. (**D**) A dose-response curve showing that SKLB188 (0–10 μM) inhibited the activity of recombinant human EGFR dose-dependently by *in vitro* kinase assay.

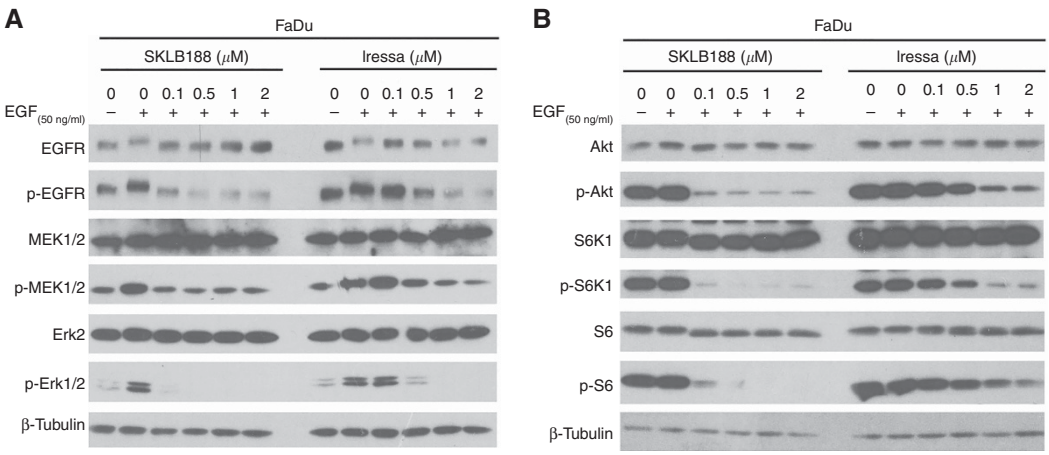

Figure 5. SKLB188 inhibits the phosphorylation of EGFR and its downstream MEK/Erk and Akt/mTOR pathways in FaDu cells. (**A** and **B**) Serum-starved FaDu cells were treated with SKLB188 (0–2 μM) or Iressa (0–2 μM) for 24 h, followed by stimulation with EGF (50 ng ml^{-1}) for 1 h. The cell lysates were subject to western blotting with indicated antibodies.

Taken together, our results indicate that SKLB188 suppresses FaDu xenograft growth in mice by inhibiting EGFR signalling, leading to inhibition of cell proliferation and induction of apoptosis of the tumour cells.

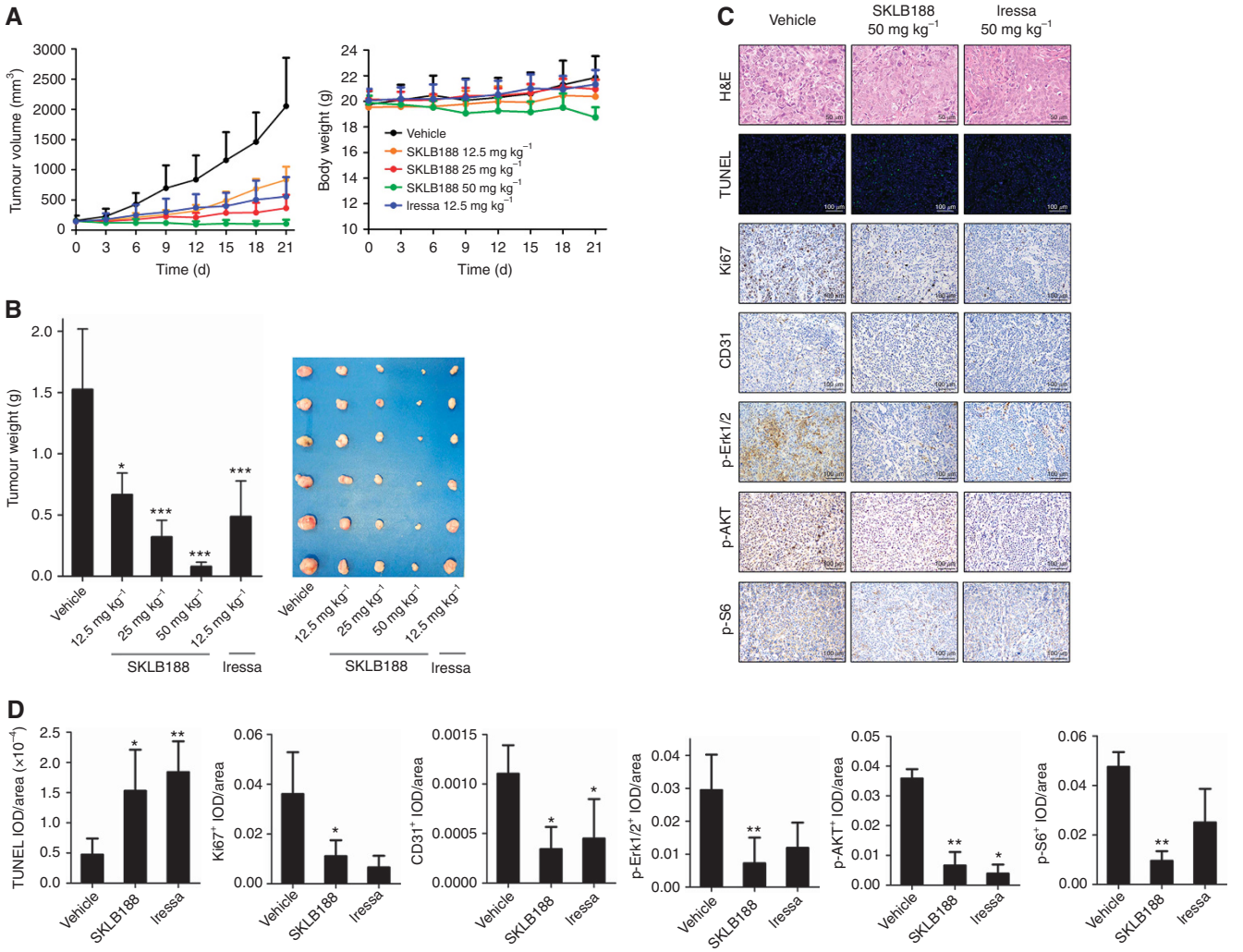

Figure 6. *In vivo* anti-tumour activity and mechanism of action of SKLB188. (**A**) Nude mice bearing FaDu tumour cells were treated with SKLB188 or Iressa at the indicated doses or vehicle control alone over 21 days. Points, mean tumour volume or mean body weight; bars, s.d. values. (**B**) At the end of the experiments, the mice were killed and the tumour tissues were dissected and weighed. The data are expressed as the mean ± s.d. of groups (6 mice per group). The representative images of isolated tumours are also shown. $*P<0.05$; $***P<0.001$. (**C**) Tumour tissues from FaDu xenografts treated with vehicle control, SKLB188 (50 mg kg^{-1}) or Iressa (50 mg kg^{-1}) for 7 days (4 mice per group) were evaluated by H&E, TUNEL, and immunohistochemistry with indicated antibodies. Representative images are shown. (**D**) Quantitative analyses for (**C**). $*P<0.05$; $**P<0.01$.

DISCUSSION

By screening an in-house focused library containing approximately 650 000 known kinase inhibitors and kinase inhibitor-like compounds containing common kinase inhibitor core scaffolds, we have identified that SKLB188 is a potential anticancer agent. Here, for the first time, we present evidence that SKLB188 exhibits potent anticancer activity against HNSCC both *in vitro* and *in vivo*, by targeting EGFR signalling.

After identifying SKLB188 inhibition of EGFR signalling, we also compared the anticancer effects of SKLB188 with Iressa (Gefitinib), a known EGFR TKI, which has been clinically used for treatment of NSCLC (Kazandjian *et al*, 2016). In the 6-day growth inhibition assay, the IC_{50} values of SKLB188 were around 10–20 nM in FaDu and PCI-13 cells (Figure 1A), whereas the IC_{50} values of Iressa were 240–400 nM in the cells, respectively (Supplementary Figure S4A). In the 72-h cell viability assay (MTS assay), the IC_{50} values of SKLB188 were approximately 0.5–1 μM in FaDu and PCI-13 cells (Figure 1B), while the IC_{50} values of Iressa were more than 2 μM in the cells (Supplementary Figure S4B). The results suggest SKLB188 inhibited cell proliferation and induced cell death of HNSCC cells more potently than Iressa *in vitro*. In line with this, we found that treatment with 0.1 μM of SKLB188 for 24 h was able to drastically inhibit EGF-stimulated phosphorylation of EGFR, MEK1/2, Erk1/2, Akt, S6K1, and S6 (Figure 5, left panel). However, similar effects were not observed until the concentration of Iressa reached to 0.5 μM (Figure 5, right panel). Therefore, the more potent *in vitro* anticancer activity of SKLB188 may be attributed to the fact that SKLB exhibited stronger inhibitory effects on the phosphorylation of EGFR and the downstream effectors (MEK1/2, Erk1/2, Akt, S6K1 and S6), compared to Iressa. In addition, we could not rule out the possibility that SKLB188 may target more kinases than Iressa. It is well known that MEK1/2-Erk1/2 and Akt-mTOR pathways are regulated not only by EGFR, but also by other RTKs (e.g., VEGFR, FGFR, etc.) (Cohen, 2014). Our *in vitro* kinase inhibition profile of SKLB188 has shown that SKLB188, at 10 μM, could inhibit EGFR and other RTKs, such as Abl, Erb2, Erb4, Flt1, Flt3, Flt4, EphB, FGFR, c-Kit, Met, and PDGFR (Supplementary Table S1). Although SKLB188 showed a much higher selectivity in

inhibiting EGFR than c-Kit ($IC_{50} = 5$ nM for EGFR *vs* 1272 nM for c-Kit), it remains to be determined whether SKLB188, at low nanomolar concentrations, inhibits other RTKs.

However, unlike the above *in vitro* data, our *in vivo* results showed that at the same dose ($12.5\,mg\,kg^{-1}$), SKLB188 did not inhibit FaDu xenograft growth more potently than Iressa, when orally administered to mice (Figure 6). Instead, a weaker inhibition was noticed. At this stage, we do not know the exact reason. Likely, this is associated with a lower bioavailability and/or quicker degradation of SKLB188 in mice. Thus, further research is required to evaluate the pharmacokinetic profile of SKLB188 in animals. Such data would be instructive to help develop derivatives of SKLB188 with improved properties in pharmacokinetics.

The first/second generation EGFR TKIs, for example, Erlotinib, Gefitinib and Afatinib, have been widely used for treatment of the advanced NSCLC patients (Barnes *et al*, 2017). However, a major handicap of these EGFR inhibitors is the rapid development of acquired resistance, most frequently due to the secondary T790M mutation within EGFR (Barnes *et al*, 2017). As such, the third-generation EGFR TKIs have emerged, which can inhibit mutant EGFR (T790M) (Jia *et al*, 2016; Skoulidis and Papadimitrakopoulou, 2017). Recently, mutation of EGFR (T790M) has been documented in HNSCC (Vatte *et al*, 2017). Of interest, apart from EGFR, ErbB2 and ErbB4 were also targeted by SKLB188 (Supplementary Table S1). Furthermore, SKLB188 was able to potently inhibit both wild-type EGFR and mutant EGFR (L858R, L861Q, T790M, and T790M/L858R) (Supplementary Table S1), suggesting that SKLB188 may have advantage over the first-/second-generation EGFR TKIs in inhibiting mutant EGFR (T790). Further studies are on the way to validate whether this is the case.

p53 is a tumour suppressor that maintains a dynamic balance between cell proliferation and cell death in response to genomic stress (Levine *et al*, 1991). Over 50% of tumours harbour somatic mutations of *TP53* gene (Kruiswijk *et al*, 2015). Recently, the Cancer Genome Atlas has demonstrated that mutation of the *TP53* gene is the most common genomic alteration identified in HNSCCs (Zhou *et al*, 2016). p53 functions as a tumour suppressor, in part by transcriptionally upregulating the expression of $p21^{Cip1}$, a CDK inhibitor, leading to cell cycle arrest in G_1 phase (Kruiswijk *et al*, 2015). FaDu cell line is *p53*-mutant (R248L) (Kim *et al*, 1993), and PCI-13 is *p53*-deficient (Zhou *et al*, 2014). Here we found that SKLB188 induced high expression of $p21^{Cip1}$ in both FaDu and PCI-13 cells, suggesting *p53*-independent induction of $p21^{Cip1}$. Our results indicate that SKLB188 has a great advantage in treating HNSCCs with *p53* mutations.

In conclusion, we have shown that SKLB188 inhibits cell proliferation and induces cell apoptosis of HNSCC cells *in vitro* and *in vivo*. SKLB188 exerts the anticancer action, at least in part, by inhibiting EGFR-mediated MEK/Erk and Akt/mTOR signalling pathways. Our findings suggest that SKLB188 is a novel EGFR inhibitor, which has a great potential for treatment of head and neck cancer and other tumours.

ACKNOWLEDGEMENTS

This work was supported in part by the grants from National Institutes of Health (NIH/NCI CA115414; to SH), American Cancer Society (RSG-08-135-01-CNE; to SH), the 973 Program (2013CB967204; to S-Y Yang), the National Natural Science Foundation of China (81325021, 81473140, and 81573349; to S-Y Yang), and the Program for Changjiang Scholars and Innovative Research Team in University (IRT13031; to S-Y Yang).

CONFLICT OF INTEREST

The authors declare no conflict of interest.

REFERENCES

Barnes TA, O'Kane GM, Vincent MD, Leighl NB (2017) Third-generation tyrosine kinase inhibitors targeting epidermal growth factor receptor mutations in non-small cell lung cancer. *Front Oncol* **7**: 113.

Chen X, Gu Y, Singh K, Shang C, Barzegar M, Jiang S, Huang S (2014) Maduramicin inhibits proliferation and induces apoptosis in myoblast cells. *PLoS One* **9**: e115652.

Chong CR, Jänne PA (2013) The quest to overcome resistance to EGFR-targeted therapies in cancer. *Nat Med* **19**: 1389–1400.

Clark CA, McEachern MD, Shah SH, Rong Y, Rong X, Smelley CL, Caldito GC, Abreo FW, Nathan CO (2010) Curcumin inhibits carcinogen and nicotine-induced mammalian target of rapamycin pathway activation in head and neck squamous cell carcinoma. *Cancer Prev Res (Phila)* **3**: 1586–1595.

Cohen RB (2014) Current challenges and clinical investigations of epidermal growth factor receptor (EGFR)- and ErbB family-targeted agents in the treatment of head and neck squamous cell carcinoma (HNSCC). *Cancer Treat Rev* **40**: 567–577.

Colevas AD (2006) Chemotherapy options for patients with metastatic or recurrent squamous cell carcinoma of the head and neck. *J Clin Oncol* **24**: 2644–2652.

Elmore S (2007) Apoptosis: a review of programmed cell death. *Toxicol Pathol* **35**: 495–516.

Furnari FB, Cloughesy TF, Cavenee WK, Mischel PS (2015) Heterogeneity of epidermal growth factor receptor signalling networks in glioblastoma. *Nat Rev Cancer* **15**: 302–310.

Guo G, Gong K, Wohlfeld B, Hatanpaa KJ, Zhao D, Habib AA (2015) Ligand-independent EGFR signaling. *Cancer Res* **75**: 3436–3441.

Jia Y, Yun CH, Park E, Ercan D, Manuia M, Juarez J, Xu C, Rhee K, Chen T, Zhang H, Palakurthi S, Jang J, Lelais G, DiDonato M, Bursulaya B, Michellys PY, Epple R, Marsilje TH, McNeill M, Lu W, Harris J, Bender S, Wong KK, Jänne PA, Eck MJ (2016) Overcoming EGFR(T790M) and EGFR(C797S) resistance with mutant-selective allosteric inhibitors. *Nature* **534**: 129–132.

Jones G, Willett P, Glen RC, Leach AR, Taylor R (1997) Development and validation of a genetic algorithm for flexible docking. *J Mol Biol* **267**: 727–748.

Kang H, Kiess A, Chung CH (2015) Emerging biomarkers in head and neck cancer in the era of genomics. *Nat Rev Clin Oncol* **12**: 11–26.

Kazandjian D, Blumenthal GM, Yuan W, He K, Keegan P, Pazdur R (2016) FDA approval of gefitinib for the treatment of patients with metastatic EGFR mutation-positive non-small cell lung cancer. *Clin Cancer Res* **22**: 1307–1312.

Keese M, Magdeburg RJ, Herzog T, Hasenberg T, Offterdinger M, Pepperkok R, Sturm JW, Bastiaens PI (2005) Imaging epidermal growth factor receptor phosphorylation in human colorectal cancer cells and human tissues. *J Biol Chem* **280**: 27826–27831.

Kim MS, Li SL, Bertolami CN, Cherrick HM, Park NH (1993) State of p53, Rb and DCC tumor suppressor genes in human oral cancer cell lines. *Anticancer Res* **13**: 1405–1413.

Kruiswijk F, Labuschagne CF, Vousden KH (2015) p53 in survival, death and metabolic health: a lifeguard with a licence to kill. *Nat Rev Mol Cell Biol* **16**: 393–405.

Leemans CR, Braakhuis BJ, Brakenhoff RH (2011) The molecular biology of head and neck cancer. *Nat Rev Cancer* **11**: 9–22.

Levine AJ, Momand J, Finlay CA (1991) The p53 tumour suppressor gene. *Nature* **351**: 453–456.

Llambi F, Green DR (2001) Apoptosis and oncogenesis: give and take in the BCL-2 family. *Curr Opin Genet Dev* **21**: 12–20.

Luo Y, Liu L, Wu Y, Singh K, Su B, Zhang N, Liu X, Shen Y, Huang S (2015) Rapamycin inhibits mSin1 phosphorylation independently of mTORC1 and mTORC2. *Oncotarget* **6**: 4286–4298.

Malumbres M, Barbacid M (2009) Cell cycle, CDKs and cancer: a changing paradigm. *Nature Rev Cancer* **9**: 153–166.

Martins RG, Parvathaneni U, Bauman JE, Sharma AK, Raez LE, Papagikos MA, Yunus F, Kurland BF, Eaton KD, Liao JJ, Mendez E,

Futran N, Wang DX, Chai X, Wallace SG, Austin M, Schmidt R, Hayes DN (2013) Cisplatin and radiotherapy with or without erlotinib in locally advanced squamous cell carcinoma of the head and neck: a randomized phase II trial. *J Clin Oncol* **31**: 1415–1421.

Odaka Y, Xu B, Luo Y, Shen T, Shang C, Wu Y, Zhou H, Huang S (2014) Dihydroartemisinin inhibits the mammalian target of rapamycin-mediated signaling pathways in tumor cells. *Carcinogenesis* **35**: 192–200.

Pezzuto F, Buonaguro L, Caponigro F, Ionna F, Starita N, Annunziata C, Buonaguro FM, Tornesello ML (2015) Update on head and neck cancer: current knowledge on epidemiology, risk factors, molecular features and novel therapies. *Oncology* **89**: 125–136.

Rodriguez CP, Adelstein DJ, Rybicki LA, Saxton JP, Lorenz RR, Wood BG, Scharpf J, Ives DI (2012) Single-arm phase II study of multiagent concurrent chemoradiotherapy and gefitinib in locoregionally advanced squamous cell carcinoma of the head and neck. *Head Neck* **34**: 1517–1523.

Scaltriti M, Baselga J (2006) The epidermal growth factor receptor pathway: a model for targeted therapy. *Clin Cancer Res* **12**: 5268–5272.

Sacco AG, Worden FP (2016) Molecularly targeted therapy for the treatment of head and neck cancer: a review of the ErbB family inhibitors. *Onco Targets Ther* **9**: 1927–1943.

Sherr CJ, Roberts JM (1999) CDK inhibitors: positive and negative regulators of G1-phase progression. *Genes Dev* **13**: 1501–1512.

Skoulidis F, Papadimitrakopoulou VA (2017) Targeting the gatekeeper: osimertinib in EGFR T790M mutation-positive non-small cell lung cancer. *Clin Cancer Res* **23**: 618–622.

van Engeland M, Nieland LJ, Ramaekers FC, Schutte B, Reutelingsperger CP (1998) Annexin V-affinity assay: a review on an apoptosis detection system based on phosphatidylserine exposure. *Cytometry* **31**: 1–9.

Vatte C, Al Amri AM, Cyrus C, Chathoth S, Acharya S, Hashim TM, Al Ali Z, Alshreadah ST, Alsayyah A, Al-Ali AK (2017) Tyrosine kinase domain mutations of EGFR gene in head and neck squamous cell carcinoma. *Onco Targets Ther* **10**: 1527–1533.

Yun CH, Boggon TJ, Li Y, Woo MS, Greulich H, Meyerson M, Eck MJ (2007) Structures of lung cancer-derived EGFR mutants and inhibitor complexes: mechanism of activation and insights into differential inhibitor sensitivity. *Cancer Cell* **11**: 217–227.

Zheng MW, Zhang CH, Chen K, Huang M, Li YP, Lin WT, Zhang RJ, Zhong L, Xiang R, Li LL, Liu XY, Wei YQ, Yang SY (2016) Preclinical evaluation of a novel orally available SRC/Raf/VEGFR2 inhibitor, SKLB646, in the treatment of triple-negative breast cancer. *Mol Cancer Ther* **15**: 366–378.

Zhou G, Liu Z, Myers JN (2016) TP53 mutations in head and neck squamous cell carcinoma and their impact on disease progression and treatment response. *J Cell Biochem* **117**: 2682–2692.

Zhou G, Wang J, Zhao M, Xie TX, Tanaka N, Sano D, Patel AA, Ward AM, Sandulache VC, Jasser SA, Skinner HD, Fitzgerald AL, Osman AA, Wei Y, Xia X, Songyang Z, Mills GB, Hung MC, Caulin C, Liang J, Myers JN (2014) Gain-of-function mutant p53 promotes cell growth and cancer cell metabolism via inhibition of AMPK activation. *Mol Cell* **54**: 960–974.

Zhou H, Shen T, Luo Y, Liu L, Chen W, Xu B, Han X, Pang J, Rivera CA, Huang S (2010) The antitumor activity of the fungicide ciclopirox. *Int J Cancer* **127**: 2467–2477.

Supplementary Information accompanies this paper on British Journal of Cancer website (http://www.nature.com/bjc)